

# Glassy properties of Anderson localization: pinning, avalanches and chaos.

G. Lemarié<sup>1,\*</sup>

<sup>1</sup>*Laboratoire de Physique Théorique, IRSAMC, Université de Toulouse, CNRS, UPS, France*  
(Dated: September 6, 2018)

I present the results of extensive numerical simulations which reveal the glassy properties of Anderson localization in dimension two at zero temperature: pinning, avalanches and chaos. I first show that the directed paths taken by the transport in the strongly localized regime are pinned by disorder and perform avalanches when a parameter like the energy is varied. I determine the roughness exponent  $\zeta = 2/3$  characterizing the wandering of these paths and find that it is the same as that of the directed polymer problem. Finally, I characterize the disorder chaos property: Two replicas with infinitesimally perturbed disorder configurations have their conductance correlation which vanishes at the thermodynamic limit. Chaos is the result of the interplay between two distinct mechanisms: a spin glass chaos effect at strong disorder characteristic of directed polymer physics and an interference effect at weak disorder characteristic of universal conductance fluctuations.

*Introduction.*— Anderson localization (AL) [1, 2] is a key mechanism of non-ergodicity in disordered *quantum* systems, with prominent examples such as the insulating state of disordered materials [3], quantum multifractality [4–7] or the absence of thermalization for many-body closed systems [8–12]. Spin glass physics is another paradigm of non-ergodic behavior which arises in *classical* disordered systems. Its study has led to important theoretical breakthroughs like the concept of spontaneous replica symmetry breaking [13] and has found applications in e.g. optimization or biology [14, 15].

There have been only few analogies drawn between these two domains. In strongly localized materials, the electron glass [16] has been much discussed in the literature [17–20]. This glassy phase arises at finite temperature in the hopping regime [21] where transport is mediated by phonons. Recently, the Anderson transition on random graphs of effective infinite dimensionality has also raised a strong interest [22–28]. There is now a consensus that the delocalized phase on trees is non-ergodic [29–32], a property related to replica symmetry breaking [31]. In this article, I address the intrinsic glassy properties of AL at zero temperature, i.e. in a fully coherent regime distinct from the electron glass problem. Moreover, I deal with a finite dimensional case  $d = 2$ , more realistic than the random graph case.

In the 2D localized regime, quantum transport is strongly inhomogeneous and takes directed paths [33–41]. Because of this, strong AL is believed to be analogous to the directed polymer (DP) problem, one of the simplest statistical physics models for which the disorder plays a quite non-trivial role as in spin glasses [42–44]. This analogy was confirmed recently by numerical simulations [36–38, 45] which showed that the fluctuations of the conductance follow the universal properties of DP. This article goes a step further by addressing the glassy properties that Anderson localization could inherit from its similarity with DP physics.

Indeed, in dimension two, it is known that the DP problem is in a glassy phase where it exhibits several

characteristic glassy properties: pinning [42], avalanches [44, 46, 47] and chaos [48–53]. Then, a DP is pinned in a configuration that does not move continuously when the system is smoothly perturbed, but sometimes makes an avalanche, i.e. jumps brutally into a very different configuration. Chaos is defined as the extreme fragility of these glassy states: an infinitesimal perturbation induces a complete reorganization of the equilibrium configurations at the thermodynamic limit. Chaos was predicted originally for spin glasses and then it was realized that DP, and more generally elastic objects pinned by disorder [42, 54], form a kind of “baby spin glass” [44, 54]. Such randomly pinned objects are relevant for many experimental situations, e.g the pinning of flux lines in superconductors [55–58].

In this letter, I present the results of extensive numerical simulations which fully take into account the non-trivial interplay between quantum interference and disorder. They reveal that the three glassy properties, pinning, avalanches and chaos, are present in Anderson localization. Chaos is however crucially affected by quantum interference effects. I have used the recursive Green’s function method [59, 60] to access efficiently the zero temperature conductance of many (up to  $\approx 7 \cdot 10^4$ ) and large (up to  $4 \cdot 10^4$  sites) 2D samples. Moreover, a method [39, 61] similar to scanning gate microscopy [60, 62] allows me to image the directed paths taken by the electron flow in the strongly localized regimes. This is complemented by a careful finite-size scaling and droplet scaling arguments.

*Zero temperature conductance.*— I consider the conductance through a scattering system described by an Anderson model [1] of size  $L \times L$ :

$$H = \sum_i \varepsilon_i a_i^\dagger a_i + t \sum_{\langle i,j \rangle} a_j^\dagger a_i + H.c. , \quad (1)$$

where  $a_i$  ( $a_i^\dagger$ ) is the annihilation (creation, resp.) operator of an electron at site  $i$  of a square lattice,  $t = 1$  is the hopping amplitude and the sum is restricted to

nearest neighbors. The site energies are independent random variables having, unless stated, a normal distribution with zero mean and standard deviation  $W$ . Such a disordered scatterer is attached to two perfect leads, which can be either wide with the same section of the sample, or narrow, consisting in a 1D lead attached at the middle of one edge. The results presented in this letter all correspond to the case of a narrow left lead and a wide right lead, but I have checked that two wide leads have qualitatively similar properties. Open boundary conditions along the transverse direction are considered.

The zero temperature dimensionless conductance at energy  $E_F$  of this model is computed through the Fisher-Lee formula [63]  $g(E_F) = \text{Tr}[\Gamma_L \mathcal{G}^r \Gamma_R \mathcal{G}^a]$ , which uses the Green's function  $\mathcal{G}(E_F)$  of the scatterer dressed by the leads, with the exponent  $r$  ( $a$ ) denoting retarded (advanced, respectively), and  $\Gamma_{L,R} = -2\text{Im}[\Sigma_{L,R}^r]$  the imaginary part of the self-energies associated to the leads, see [59]. The Green's function is efficiently calculated numerically using the recursive Green's function approach [59].

*Analogy with the directed polymer problem.*— Before describing the analysis of the glassy properties of zero temperature transport, I briefly review the analogy with the DP problem and the recent numerical studies supporting it. The Green's function element between a point  $A$  at the left edge of the scatterer and another point  $B$  at the right edge can be expressed formally using the locator expansion [1]:

$$\mathcal{G}_{A,B}(E_F) = \sum_{\mathcal{P}} \prod_{i \in \mathcal{P}} \frac{1}{E_F - \varepsilon_i} \quad (2)$$

where the sum is over all paths  $\mathcal{P}$  connecting  $A$  to  $B$  and the product is over all sites belonging to path  $\mathcal{P}$ . In the strongly localized regime, the weight  $\prod_{i \in \mathcal{P}} (E_F - \varepsilon_i)^{-1}$  of a path  $\mathcal{P}$  will decrease exponentially with its length. The sum over paths will then be dominated by the forward-scattering paths which propagate from left to right [33–40]. One thus obtains a mapping to the DP problem in dimension two where the partition function of the DP  $Z = \sum_{\mathcal{DP}} \prod_{i \in \mathcal{DP}} e^{-\beta V_i}$  corresponds to the Green's function expansion (2) with on-site disorder  $V_i = \ln(E_F - \varepsilon_i)$  and inverse temperature  $\beta = 1$ .

Using this analogy and the universality of the physics of DP [42, 65], one can understand a certain number of properties of conductance fluctuations in the localized regime in dimension two [36–38, 45]: The logarithm of the conductance  $\ln g$  is analogous to minus the free-energy of the DP problem and follows in the strongly localized regime:  $\ln g = -2L/\xi + \alpha (L/\xi)^\theta \chi$ , with  $\xi$  the localization length,  $\theta = 1/3$  the *universal* value expected in the DP problem in dimension  $d = 2$  and  $\chi$  a random variable of order one with the Tracy-Widom distribution.

*Pinning and avalanches.*— I now address the glassy properties of the strongly localized regime on the light

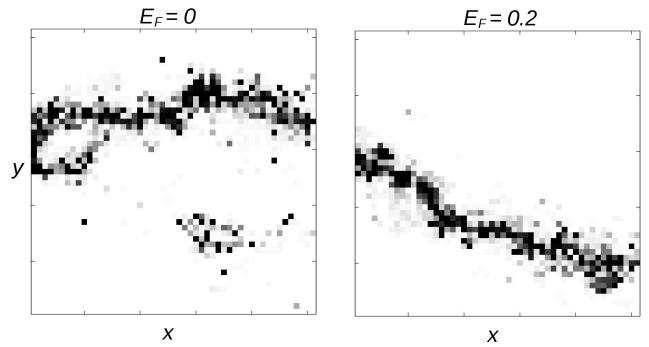


FIG. 1. In the Anderson localized regime, the zero temperature transport is strongly inhomogeneous and takes place along certain directed paths [39]. Similarly to scanning gate microscopy [64], a gray scale plot of the change of conductance  $|g(i) - g_0|/g_0$ , where  $g(i)$  is the conductance of the sample with  $\varepsilon_i \rightarrow -\varepsilon_i$  and  $g_0$  the unperturbed conductance, allows to image the path taken by the electron flow [61]. A single sample with a box-distributed disorder  $W = 20$  and size  $L = 50$  is considered at two values of the energy  $E_F$ .

of the analogy with the DP problem. In the strongly localized regime  $\xi \ll L$ , the electron flow is very inhomogeneous, and follows directed paths [37, 39] which correspond to the dominant paths of the DP problem [42]. It is possible to visualize such paths by considering how the conductance of a sample is affected when one changes the on-site energy  $\varepsilon_i$  of site  $i$  by its opposite value  $-\varepsilon_i$  [39, 61]. Thus, as seen in fig. 1, by representing in a color plot  $|g(i) - g_0|/g_0$  as a function of the site position  $i$ , where  $g_0$  is the conductance of the sample without perturbation, and  $g(i)$  the conductance of the sample locally perturbed in  $i$ , the flow of electron is visualized. This method is similar to Scanning Gate Microscopy [64], where branched electron flow was observed experimentally in smoothly correlated disordered systems. Moreover, it corresponds in the DP problem, to the response of the free energy to an infinitesimal perturbation of the energy of a site. In this case, one can prove [66] that it gives exactly the probability that the polymer passes on the site.

Using this approach, one can observe clearly pinning of the electron flow and avalanches between different directed paths when varying a parameter such as the energy  $E_F$ . In fig. 2, I represent the transverse position  $\langle y \rangle$  of the path at the right end of the disordered sample:

$$\langle y \rangle \equiv \frac{1}{\mathcal{N}} \sum_y (y - L/2) \frac{|g(x = L, y) - g_0|}{g_0}, \quad (3)$$

with  $\mathcal{N} = \sum_y |g(x = L, y) - g_0|/g_0$ , as a function of  $E_F$ . One can clearly observe plateaus which are the signature of pinning, with brutal jumps at certain values of  $E_F$  which depend on the microscopic disorder configuration. Thus, in the case of fig. 1, the path taken by the electron flow remains the same as that of the left panel between  $E_F = 0$  and  $E_F = 0.1$  and suddenly jumps to the path

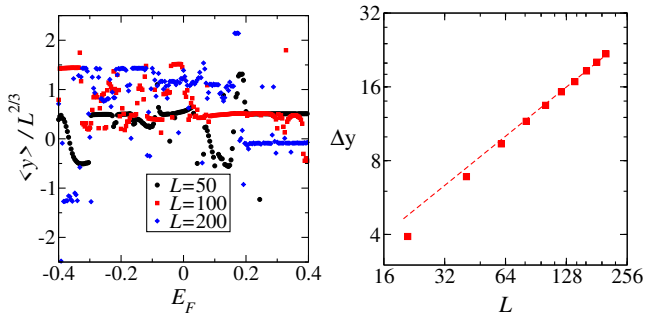


FIG. 2. Pinning and avalanches of Anderson localization. *Left*: Similarly to DP, glassy properties arise from the sensitivity of the path taken by transport to a perturbation, such as a slight change of the energy  $E_F$ . The final position of the path  $\langle y \rangle$  (see text) is pinned most of the time but jumps abruptly to a very different value. These (equilibrium) avalanches make a brutal change between different paths such as those represented in Fig. 1. The parameters are the same as in Fig. 1. *Right*: Pinning can be characterized by the roughness exponent  $\zeta$  defined as  $\Delta y = \sqrt{\langle y \rangle^2} \sim L^\zeta$ . For the DP problem  $\zeta = 2/3$  is exactly known. This behavior is represented by the red dashed line and agrees well with numerical data for the Anderson model with a normal distribution,  $W = 15$ , and averaging over 18000 samples. The typical size of the jumps  $\Delta y$  in the left panel is controlled by the roughness exponent.

of the right panel at  $E_F = 0.1$  up to  $E_F = 0.2$ .

In the DP problem, pinning is characterized by the roughness exponent  $\zeta$  which measures the wandering of the DP:  $\zeta$  is defined through  $\langle y \rangle^2 \sim L^{2\zeta}$  for a point-like initial condition starting at  $y = L/2$  for  $x = 0$  ( $\bar{X}$  means disorder averaging of  $X$ ). In dimension  $d = 2$ , the critical exponent  $\zeta = 2/3$  is known exactly. The fig. 2, right panel, represents the evolution with system size of  $\Delta y = \sqrt{\langle y \rangle^2}$  for the 2D AL problem. The numerical data agree well with the DP value  $\zeta = 2/3$ . Moreover, in the left panel of fig. 2, the typical size of the equilibrium avalanche jumps is seen to scale as  $\Delta y \sim L^{2/3}$ , as expected for the DP problem [44]. Together with  $\theta = 1/3$  [36–38], the value of the critical exponent  $\zeta = 2/3$  confirms that 2D AL belongs to the same universality class as that of the DP problem.

*Chaos.*— I now turn to the spectacular glassy effect known as chaos [48–53]. I show that two replicas of the Anderson model, infinitesimally perturbed with respect to each other, have completely uncorrelated conductances at the thermodynamic limit, i.e. the conductance is fragile. In close analogy with the disorder chaos effect in spin glasses and DP, I study the change of the conductance under a perturbation of the disorder configuration:

$$\varepsilon_i^\delta = \frac{\varepsilon_i + \delta \varepsilon'_i}{\sqrt{1 + \delta^2}}. \quad (4)$$

Here,  $\varepsilon$  and  $\varepsilon'$  are both normally distributed with the

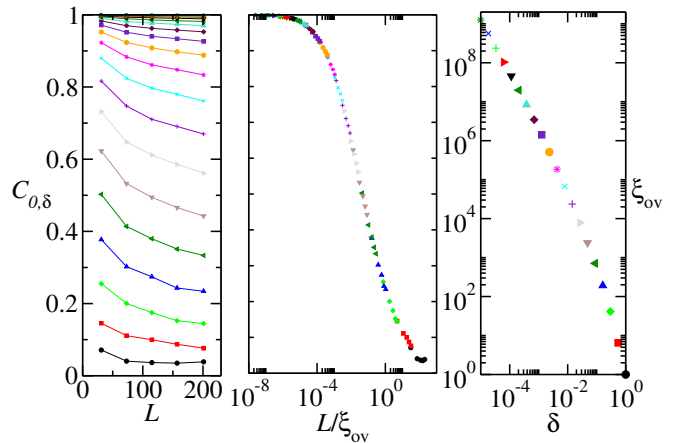


FIG. 3. Disorder chaos of Anderson localization. The correlation function of  $\ln g$  with a perturbation of the disorder configuration (4) characterized by the parameter  $\delta$  is plotted as a function of system size  $L$  in the left panel (decreasing  $\delta$  from upper to lower curves). The middle panel shows the single parameter scaling of  $C_{0,\delta}(L)$  as a function of the overlap length  $\xi_{ov}(\delta)$ . This scaling function shows that an infinitesimal perturbation induces large changes in the conductance so that  $C_{0,\delta}(L)$  vanishes for  $L \gg \xi_{ov}$ . The divergence of  $\xi_{ov}$  as a function of  $\delta$  is shown in the right panel. 72000 disordered 2D samples connected to a narrow left lead and a wide right lead have been considered for each values of  $\delta$  and  $L$ , with a disorder strength  $W = 10$  and  $E_F = 0.01$ .

same mean 0 and standard deviation  $W$  and  $\delta$  denotes the strength of the perturbation. I consider the correlation function of the logarithm of the conductance between the two replicas:

$$C_{0,\delta}(L) = \frac{\overline{\Delta \ln g_\delta \Delta \ln g_0}}{\sqrt{\overline{\Delta \ln g_\delta^2} \overline{\Delta \ln g_0^2}}}, \quad (5)$$

where  $\Delta \ln g \equiv \ln g - \overline{\ln g}$ .

In the left panel of fig. 3,  $C_{0,\delta}(L)$  is represented as a function of the system size  $L$  for different values of the perturbation strength  $\delta$ . In the limit of small  $\delta$  (upper curves), the two replicas are strongly correlated,  $C_{0,\delta} \approx 1$  with a very slow decrease as a function of  $L$ . On the other hand, at large  $\delta$ , the correlation is vanishing. The middle panel shows that all the data collapse onto a single curve when plotted as a function of  $L/\xi_{ov}$ , with  $\xi_{ov}$  known as the overlap length. This scaling behavior supports the chaos property of AL: an infinitesimal perturbation induces a vanishing correlation for  $L \gg \xi_{ov}$ .

The overlap length  $\xi_{ov}$  depends only on  $\delta$  and is shown in the right panel of fig. 3. In the DP problem, its divergence can be understood from a droplet scaling argument [51, 52]. To this end, I consider the case of a DP with real on-site energies  $V_i = \ln |\varepsilon_i|$  (such an argument is not available for complex  $V_i = \ln(E_F - \varepsilon_i)$ ) with  $E_F = 0$ . The scaling argument compares the energy cost of remaining in the same path in the perturbed replica with

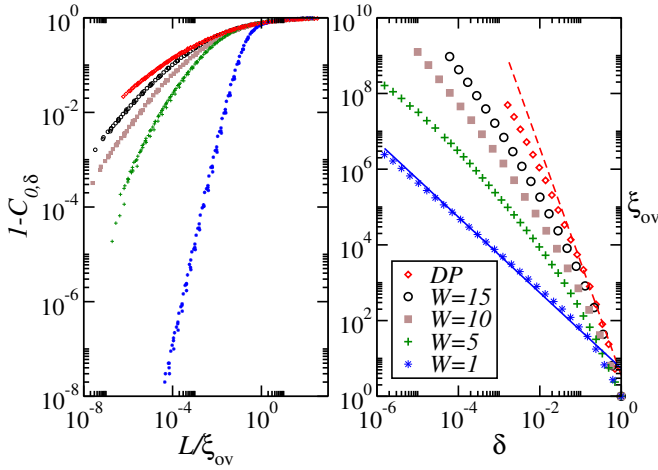


FIG. 4. Disorder chaos of Anderson localization for different disorder strengths  $W$ . The scaling function and the overlap length divergence depend crucially on the disorder strength, contrary to the case of the DP problem. The red dashed line corresponds to the droplet scaling prediction  $\xi_{ov} \sim \delta^{-3}$ , which agrees well with the DP data and the AL data at strong disorder and not too small  $\delta$ . The blue line indicates the expected behavior in the weak localization regime  $\xi_{ov} \sim \delta^{-1}$  (see text), which agrees well with the data at  $W = 1$  for small values of  $\delta$ . Otherwise, identical to fig. 3

the free-energy gain to jump into another configuration  $\Delta F \sim L^{1/3}$ . Here, the energy cost can be written as:

$$\Delta E = \sum_{i=1}^L \ln(|\varepsilon_i^\delta|) - \ln(|\varepsilon_i|) = \sum_{i=1}^L \ln \frac{|1 + \delta \frac{\varepsilon_i'}{\varepsilon_i}|}{\sqrt{1 + \delta^2}}, \quad (6)$$

where the sum is along the sites of the dominant path. While  $\varepsilon_i$  are correlated random variables (the dominant path is the result of a global optimization of the energy cost of a path), the perturbed  $\varepsilon_i'$  are uncorrelated, and the total term in the log is therefore uncorrelated. A simple calculation shows that the variable  $\ln |1 + \delta \varepsilon_i'/\varepsilon_i|$  has a finite average value  $\ln \sqrt{1 + \delta^2}$  and a standard deviation  $\sigma \propto \sqrt{\delta}$ . According to the central limit theorem:  $\Delta E \sim \sqrt{\delta L}$ . Because  $\Delta E$  and  $\Delta F$  do not vary with the same power laws with  $L$ , at small  $\delta$  and small system size  $L \ll \xi_{ov}$ ,  $\Delta E$  is smaller than  $\Delta F$  and the two replicas are in the same configurations, whereas for large system sizes  $L \gg \xi_{ov}$ , the perturbation has made the path jump into a completely different configuration and the replicas are uncorrelated. The overlap length is such that  $\delta^{1/2} \xi_{ov}^{1/2} \sim \xi_{ov}^{1/3}$ , therefore  $\xi_{ov} \sim \delta^{-3}$ . In fig. 4, I represent the disorder chaos effect on such DP with  $V_i = \ln |\varepsilon_i|$  (diamonds points). There is a good agreement between the data for  $\xi_{ov}$  and the prediction of the droplet scaling argument (red dashed line).

While AL data are quite close to the DP results at the strongest disorder  $W = 15$  I could consider (see the open circles data in fig. 4), a striking observation of fig. 4 is however that disorder chaos for AL depends crucially

on the disorder strength  $W$ , with a stronger fragility as  $W$  decreases from 15 to 1. The strong fragility at small disorder  $W = 1$  corresponds to the famous universal conductance fluctuations [67–69]. Indeed, in the weak localization regime, the conductance results from the interference between many multiply scattered Feynman paths (instead of one main path as before) and thus crucially depends on their relative phases. These phases can be altered by a perturbation. In the case of a change of  $E_F$  by  $\omega$  between the two replicas, a pair of identical Feynman paths dephases by an amount  $\omega t_P/\hbar$  where  $t_P$  is the time to travel the path. In the diffusive regime, the typical value of  $t_P \propto E_{Th}^{-1}$  with  $E_{Th} = \hbar D/L^2$  the Thouless Energy,  $D$  the diffusion constant. Therefore, the overlap length follows  $\xi_{ov} \sim \omega^{-1/2}$ . In the present case of a disorder perturbation (4), the dephasing is proportional to  $\delta \sqrt{t_P}$  due to *random* shifts of alternative signs (instead of the constant shift  $\omega$ ) of the on-site energies. This explains the observed behavior  $\xi_{ov} \sim \delta^{-1}$ , shown by the blue line in the right panel of fig. 4.

The observations of fig. 4 are therefore quite different from the DP problem for which the chaos effect does not depend on the strength of disorder [52]. Interestingly, the chaos property of AL results from the interplay between two distinct mechanisms: an interference effect between many paths which dominates in the weak localization regime [67], and the glassy chaos effect of the DP problem at strong disorder which brutally changes the directed path taken by the transport. Let me stress that this subtle interplay persists at large scales, since it is the scaling function associated to chaos that depends on  $W$ .

*Experimental observations.*— The glassy effects described here could be observed experimentally in several types of systems such as two-dimensional electron gases [2, 70], cold atom systems, or classical waves. e.g. microwaves [71] or ultrasounds [72]. In two-dimensional electron gases, scanning gate microscopy [62] could image the directed paths associated with AL. In cold atomic gases, AL has been characterized in a very controlled manner [73–76]. Very recently, an experimental approach to study the conductance in cold atoms has been developed [77], which allows the introduction of disorder [78] and scanning gate microscopy imaging [79].

*Conclusion.*— In this article, I have shown from extensive numerical simulations that AL in two dimensions and at zero temperature satisfies several important glassy properties inherited from DP physics but where quantum interference effects play a crucial role: pinning, avalanches, and chaos. AL opens a new playground for the study of quantum glassy physics.

It would be particularly interesting to see whether these glassy properties extend to the case of interacting systems. The method of analysis presented here could in particular help to clarify the glassy nature of the Bose glass insulating phase of disordered bosons [80–86].

This paper is dedicated to the memory of Jean-

Louis Pichard. I thank C. Castellani, B. Georgeot, F. Pietracaprina and T. Thiery for useful comments on the manuscript. I thank also M. Dupont, N. Laflorence, C. Monthus and A. Rosso for interesting discussions. I thank CalMiP for access to its supercomputer. This work was supported by Programme Investissements d'Avenir under the program ANR-11-IDEX-0002-02, reference ANR-10-LABX-0037-NEXT, and the ANR grant COCOA No ANR-17-CE30-0024-01.

---

\* Corresponding author: lemari@irsamc.ups-tlse.fr

- [1] P. W. Anderson, Phys. Rev. **109**, 1492 (1958).
- [2] E. Abrahams, *50 years of Anderson Localization* (World Scientific, 2010).
- [3] V. Dobrosavljevic, N. Trivedi, and J. M. Valles Jr, *Conductor insulator quantum phase transitions* (Oxford University Press, 2012).
- [4] C. Castellani and L. Peliti, J. Phys. A **19**, L429 (1986).
- [5] F. Wegner, Z. Phys. B **36**, 209 (1980).
- [6] F. Evers and A. D. Mirlin, Rev. Mod. Phys. **80**, 1355 (2008).
- [7] M. Feigel'Man, L. Ioffe, V. Kravtsov, and E. Cuevas, Ann. Phys. **325**, 1390 (2010).
- [8] B. L. Altshuler, Y. Gefen, A. Kamenev, and L. S. Levitov, Phys. Rev. Lett. **78**, 2803 (1997).
- [9] D. Basko, I. Aleiner, and B. Altshuler, Ann. Phys. **321**, 1126 (2006).
- [10] I. V. Gornyi, A. D. Mirlin, and D. G. Polyakov, Phys. Rev. Lett. **95**, 206603 (2005).
- [11] R. Nandkishore and D. A. Huse, Annu. Rev. Condens. Matter Phys. **6**, 15 (2015).
- [12] D. A. Abanin, E. Altman, I. Bloch, and M. Serbyn, arXiv preprint arXiv:1804.11065 (2018).
- [13] M. Mézard, G. Parisi, and M. Virasoro, *Spin glass theory and beyond: An Introduction to the Replica Method and Its Applications*, Vol. 9 (World Scientific Publishing Co Inc, 1987).
- [14] A. P. Young, *Spin glasses and random fields*, Vol. 12 (World Scientific, 1998).
- [15] D. L. Stein and C. M. Newman, *Spin glasses and complexity* (Princeton University Press, 2013).
- [16] J. Davies, P. Lee, and T. Rice, Phys. Rev. Lett. **49**, 758 (1982).
- [17] M. Müller and L. B. Ioffe, Phys. Rev. Lett. **93**, 256403 (2004).
- [18] A. M. Somoza, M. Ortuño, M. Caravaca, and M. Pollak, Phys. Rev. Lett. **101**, 056601 (2008).
- [19] A. Vaknin, Z. Ovadyahu, and M. Pollak, Phys. Rev. Lett. **84**, 3402 (2000).
- [20] A. Amir, Y. Oreg, and Y. Imry, Annu. Rev. Condens. Matter Phys. **2**, 235 (2011).
- [21] M. Pollak and B. Shklovskii, *Hopping transport in solids*, Vol. 28 (Elsevier, 1991).
- [22] C. Monthus and T. Garel, J. Phys. A **42**, 075002 (2008).
- [23] G. Biroli, A. Ribeiro-Teixeira, and M. Tarzia, arXiv preprint arXiv:1211.7334 (2012).
- [24] A. De Luca, L. Altshuler, B., E. Kravtsov, V., and A. Scardicchio, Phys. Rev. Lett. **113**, 046806 (2014).
- [25] V. Kravtsov, I. Khaymovich, E. Cuevas, and M. Amini, New J. Phys. **17**, 122002 (2015).
- [26] K. Tikhonov, A. Mirlin, and M. Skvortsov, Phys. Rev. B **94**, 220203 (2016).
- [27] I. García-Mata, O. Giraud, B. Georgeot, J. Martin, R. Dubertrand, and G. Lemarié, Phys. Rev. Lett. **118**, 166801 (2017).
- [28] G. Biroli and M. Tarzia, arXiv preprint arXiv:1706.02655 (2017).
- [29] K. Tikhonov and A. Mirlin, Phys. Rev. B **94**, 184203 (2016).
- [30] D. Facchetti, P. Vivo, and G. Biroli, Europhys. Lett. **115**, 47003 (2016).
- [31] V. Kravtsov, B. Altshuler, and L. Ioffe, Ann. Phys. (2017).
- [32] M. Sonner, K. Tikhonov, and A. Mirlin, Phys. Rev. B **96**, 214204 (2017).
- [33] V. Nguyen, B. Spivak, and B. Shklovskii, Sov. Phys. JETP **62**, 1021 (1985).
- [34] H. Fritzsche and M. Pollak, *Hopping and related phenomena*, Vol. 2 (World Scientific, 1990).
- [35] E. Medina, M. Kardar, Y. Shapir, and X. R. Wang, Phys. Rev. Lett. **62**, 941 (1989).
- [36] J. Prior, A. Somoza, and M. Ortuño, Phys. Rev. B **72**, 024206 (2005).
- [37] A. M. Somoza, M. Ortuño, and J. Prior, Phys. Rev. Lett. **99**, 116602 (2007).
- [38] J. Prior, A. Somoza, and M. Ortuño, Eur. Phys. J. B **70**, 513 (2009).
- [39] P. Markoš, Physica B **405**, 3029 (2010).
- [40] F. Pietracaprina, V. Ros, and A. Scardicchio, Phys. Rev. B **93**, 054201 (2016).
- [41] E. Medina and M. Kardar, Phys. Rev. B **46**, 9984 (1992).
- [42] T. Halpin-Healy and Y.-C. Zhang, Phys. Rep. **254**, 215 (1995).
- [43] B. Derrida and H. Spohn, J. Stat. Phys. **51**, 817 (1988).
- [44] M. Mézard, J. Phys. (Paris) **51**, 1831 (1990).
- [45] A. M. Somoza, P. Le Doussal, and M. Ortuño, Phys. Rev. B **91**, 155413 (2015).
- [46] P. Jögi and D. Sornette, Phys. Rev. E **57**, 6936 (1998).
- [47] T. Thiery, arXiv preprint arXiv:1705.07457 (2017).
- [48] S. R. McKay, A. N. Berker, and S. Kirkpatrick, Phys. Rev. Lett. **48**, 767 (1982).
- [49] A. J. Bray and M. A. Moore, Phys. Rev. Lett. **58**, 57 (1987).
- [50] D. S. Fisher and D. A. Huse, Phys. Rev. B **38**, 386 (1988).
- [51] D. S. Fisher and D. A. Huse, Phys. Rev. B **43**, 10728 (1991).
- [52] M. Sales and H. Yoshino, Phys. Rev. E **65**, 066131 (2002).
- [53] R. A. da Silveira and J.-P. Bouchaud, Phys. Rev. Lett. **93**, 015901 (2004).
- [54] L. Balents, J.-P. Bouchaud, and M. Mézard, J. Phys. I **6**, 1007 (1996).
- [55] D. S. Fisher, M. P. A. Fisher, and D. A. Huse, Phys. Rev. B **43**, 130 (1991).
- [56] T. Giamarchi and P. Le Doussal, Phys. Rev. B **52**, 1242 (1995).
- [57] T. Giamarchi and P. Le Doussal, Phys. Rev. Lett. **72**, 1530 (1994).
- [58] T. Giamarchi and P. Le Doussal, Phys. Rev. B **55**, 6577 (1997).
- [59] S. Datta, *Electronic transport in mesoscopic systems* (Cambridge university press, 1997).
- [60] A. Abbout, G. Lemarié, and J.-L. Pichard, Phys. Rev. Lett. **106**, 156810 (2011).

- [61] J.-L. Pichard, in *Quantum Coherence in Mesoscopic Systems*, edited by B. Kramer, NATO ASI Series B254 (Plenum, New York) (1991).
- [62] M. Topinka, B. LeRoy, R. Westervelt, S. Shaw, R. Fleischmann, E. Heller, K. Maranowski, and A. Gossard, *Nature* **410**, 183 (2001).
- [63] D. S. Fisher and P. A. Lee, *Phys. Rev. B* **23**, 6851 (1981).
- [64] M. Topinka, B. LeRoy, R. Westervelt, S. Shaw, R. Fleischmann, E. Heller, K. Maranowski, and A. Gossard, *Nature* **410**, 183 (2001).
- [65] T. Gueudre, P. Le Doussal, J.-P. Bouchaud, and A. Rosso, *Phys. Rev. E* **91**, 062110 (2015).
- [66] C. Maes and T. Thiery, *J. Stat. Phys.* **168**, 937 (2017).
- [67] E. Akkermans and G. Montambaux, *Mesoscopic Physics of Electrons and Photons* (Cambridge University Press, Cambridge, 2007).
- [68] P. A. Lee, A. D. Stone, and H. Fukuyama, *Phys. Rev. B* **35**, 1039 (1987).
- [69] A. Altland, *Ann. Phys. (Germany)* **506**, 28 (1994).
- [70] G. Bergmann, *Phys. Rep.* **107**, 1 (1984).
- [71] A. Z. Genack and J. Wang, *Int. J. Mod. Phys. B* **24**, 1950 (2010).
- [72] A. Lagendijk, B. van Tiggelen, and D. Wiersma, *Physics Today* **62**, 24 (2009).
- [73] L. Sanchez-Palencia and M. Lewenstein, *Nat. Phys.* **6**, 87 (2010).
- [74] A. Aspect and M. Inguscio, *Physics Today* **62**, 30 (2009).
- [75] M. Lopez, J.-F. Clément, G. Lemarié, D. Delande, P. Szriftgiser, and J. C. Garreau, *New J. Phys.* **15**, 065013 (2013).
- [76] I. Manai, J.-F. m. c. Clément, R. Chicireanu, C. Hainaut, J. C. Garreau, P. Szriftgiser, and D. Delande, *Phys. Rev. Lett.* **115**, 240603 (2015).
- [77] S. Krinner, T. Esslinger, and J.-P. Brantut, *J. Phys. Condens. Matter* **29**, 343003 (2017).
- [78] S. Krinner, D. Stadler, J. Meineke, J.-P. Brantut, and T. Esslinger, *Phys. Rev. Lett.* **115**, 045302 (2015).
- [79] S. Häusler, S. Nakajima, M. Lebrat, D. Husmann, S. Krinner, T. Esslinger, and J.-P. Brantut, *Phys. Rev. Lett.* **119**, 030403 (2017).
- [80] M. P. A. Fisher, P. B. Weichman, G. Grinstein, and D. S. Fisher, *Phys. Rev. B* **40**, 546 (1989).
- [81] T. Giamarchi and H. J. Schulz, *Phys. Rev. B* **37**, 325 (1988).
- [82] E. Altman, Y. Kafri, A. Polkovnikov, and G. Refael, *Phys. Rev. Lett.* **100**, 170402 (2008).
- [83] E. V. H. Doggen, G. Lemarié, S. Capponi, and N. Laflorencie, *Phys. Rev. B* **96**, 180202 (2017).
- [84] M. Müller, *Europhys. Lett.* **102**, 67008 (2013).
- [85] A. Gangopadhyay, V. Galitski, and M. Müller, *Phys. Rev. Lett.* **111**, 026801 (2013).
- [86] C. Monthus and T. Garel, *J. Stat. Mech.* **2012**, P01008 (2012).